Energy transfer mechanism and Auger effect in Er^{3+} coupled silicon nanoparticle samples

A. Pitanti,[1,2,a] D. Navarro-Urrios,[3] N. Prtljaga,[1] N. Daldosso,[1] F. Gourbilleau,[4] R. Rizk,[4] B. Garrido,[3] and L. Pavesi[1]
[1]*Department of Physics, Nanoscience Laboratory, University of Trento, via Sommarive 14, Trento 38100, Italy*
[2]*NEST, Scuola Normale Superiore, Istituto di nanoscienze-CNR, Piazza San Silvestro 12, 56127 Pisa, Italy*
[3]*Dept. Electrònica, MIND-IN2UB, Universitat de Barcelona, Martí i Franquès 1, 08028 Barcelona, CAT, Spain*
[4]*CIMAP, UMR CEA/CNRS/ENSICAEN/Univ. CAEN, No. 6252 ENSICAEN, 6 Boulevard Maréchal Juin, 14050 Caen Cedex 4, France*

(Received 1 December 2009; accepted 14 July 2010; published online 13 September 2010)

We report a spectroscopic study about the energy transfer mechanism among silicon nanoparticles (Si-np), both amorphous and crystalline, and Er ions in a silicon dioxide matrix. From infrared spectroscopic analysis, we have determined that the physics of the transfer mechanism does not depend on the Si-np nature, finding a fast (<200 ns) energy transfer in both cases, while the amorphous nanoclusters reveal a larger transfer efficiency than the nanocrystals. Moreover, the detailed spectroscopic results in the visible range here reported are essential to understand the physics behind the sensitization effect, whose knowledge assumes a crucial role to enhance the transfer rate and possibly employing the material in optical amplifier devices. Joining the experimental data, performed with pulsed and continuous-wave excitation, we develop a model in which the internal intraband recombination within Si-np is competitive with the transfer process via an Auger electron-"recycling" effect. Posing a different light on some detrimental mechanism such as Auger processes, our findings clearly recast the role of Si-np in the sensitization scheme, where they are able to excite very efficiently ions in close proximity to their surface. © *2010 American Institute of Physics*. [doi:10.1063/1.3476286]

I. INTRODUCTION

The rare earth erbium oxides have played an important role as active material for optical amplification in the last decades;[1] the sharp, long-lifetime emission (~5–10 ms) in the third telecom window makes it the perfect candidate to be employed in all-optical amplifier. In fact, erbium doped fiber amplifier has reached a leading position in optical amplification technology. For these reasons, any improvements of the system are quite appealing and have developed an intensive research toward the use of sensitizers in Er-doped materials.[2] Indeed, the use of suitable sensitizers relaxes the expensive pumping condition of sharp-line and powerful laser diode, allows miniaturizing the system into photonic lightwave circuits and even leads to the realization of electrical injected Er doped amplifiers. Among the other sensitizers, an energy transfer mechanism has been demonstrated among Si-nanoparticles (Si-np) and Er ions.[3] Si-np present various interesting properties as sensitizers: the most important is the increase in the Er^{3+} effective excitation cross section from 10^{-20}–10^{-21} to 10^{-16}–10^{-17} cm^2 when the ions are placed in close proximity to the sensitizer.[4] This results from the the large and spectrally broad absorption cross section of the nanoparticles in the visible. Moreover, indirect excitation of Er ions by energy transfer from Si-np which, in turn, were excited by electrical injection, has been demonstrated.[5] All these appealing properties open the route to the realization of compact Er-doped sensitized waveguide amplifiers and lasers, which could be either optically or electrically pumped.

After the first encouraging results of internal optical gain in Si-nc:Er codoped SiO_2 waveguides,[6] several reports in the last years have defined intrinsic material limits to the population inversion condition, mainly imposed by an Auger back-transfer mechanism.[7,8] A widely spread believe is that this kind of mechanism is the main cause for the low fraction (~3–5%) of optically active Er ions population effectively coupled to Si-np reported so far in the literature.[9–12]

In this study, we report spectroscopic experiments performed in samples where the coupled Er content is about 52% of the optically active ions (i.e., 13.5% of total Er^{3+} concentration) (Ref. 13) and the measured internal optical gain in active waveguides is as large as 1 dB/cm.[14] The aim of this work is to investigate the energy transfer process between Si nanocrystals or Si amorphous nanoclusters and Er ions in a silicon dioxide matrix. This work complements the brief report we published recently[15] where we demonstrated the existence of a very fast and effective transfer process and the total absence of Auger back transfer. Here we provide new data where we show that the different nature of Si-np (crystalline or amorphous), while changing the transfer process efficiency, does not change the physics behind the transfer mechanism itself. Based on these experimental findings, we develop a coupled rate equation model where intraband recombinations in the Si-np play a fundamental role in the

[a]Electronic mail: pitanti@science.unitn.it.

TABLE I. Set of samples under study. Si excess (Si exc) and Er^{3+} concentration have been measured, respectively, by x-ray photoelectron spectroscopy (XPS) and secondary ion mass spectrometry (SIMS) technique. The annealing time was of one hour at the annealing temperature reported (T_{ann}).

Sample	Si exc (%)	$[Er^{3+}]$ (cm^{-3})	T_{ann} (°C)
A	5 ± 2	$3.38\pm0.2\times10^{20}$	900
B	6.3 ± 2	⋯	900
A-re	5 ± 2	$3.38\pm0.2\times10^{20}$	900+1100
B-re	6.3 ± 2	⋯	900+1100
C	⋯	$0.5\pm0.1\times10^{20}$	⋯

transfer process. In addition, we identified the transfer mechanism as a Dexter-like process.[16] In particular, a "carrier-recycling" effect due to Auger recombination within the Si-np is proposed. We used the term "recycling" since the excited carriers which are involved in the Auger process are at the same time rehabilitated to participate to the transfer process. In this perspective, the main and, possibly, only detrimental issue in achieving a complete inversion of Er^{3+} population for amplification purposes is given by the effective interaction distance between sensitizers and ions, as recently reported in literature.[11,12,17,18]

II. MATERIAL AND METHODS

The samples under study have been fabricated by a novel rf reactive magnetron cosputtering under argon–hydrogen mixture of 2 in. confocal pure SiO_2 and Er_2O_3 targets.[19] To form nanoparticles, a substochiometric silicon rich silicon oxide (SRSO) is deposited followed by an annealing treatment to ensure phase separation between silicon and its oxide. In order to perform comparative spectroscopic characterization, the deposition parameters[20] employed to obtain the best sample in terms of photoluminescence (PL) intensity (under nonresonant pumping—476 nm) and lifetime of the $^4I_{13/2}\rightarrow{}^4I_{15/2}$ Er^{3+} transition, have been used to fabricate a set of different samples with and without Er^{3+} and with different annealing treatments, (Table I). Samples A and B likely contain Si amorphous nanocluster due to the low annealing temperature used which does not allow a complete phase separation and recrystallization of Si from the matrix.[21,22] This is confirmed by their broad luminescence spectra (see more later). Pieces of these samples, named A-re and B-re, respectively, have been annealed a second time at an higher temperature of 1100 °C. It is well known that for annealing temperature of 1100 °C crystalline nanoparticles form. All samples have the same layered structure, composed of a 5 μm SiO_2 cladding layer above a Si substrate, on which is further deposited the 1.2 μm thick active material. As reference for Er^{3+} emission, we have used an Er-doped soda-lime glass fabricated by Corning (sample C).

The spectroscopic experiments have been performed both in visible (VIS) and near-infrared (IR) range, with continuous-wave (CW) and pulsed laser excitation sources. The CW source was an Ar^+ laser of which we have employed lines which were resonant (488 nm) or nonresonant (476 nm) with Er^{3+} internal transitions.[1] The average photon

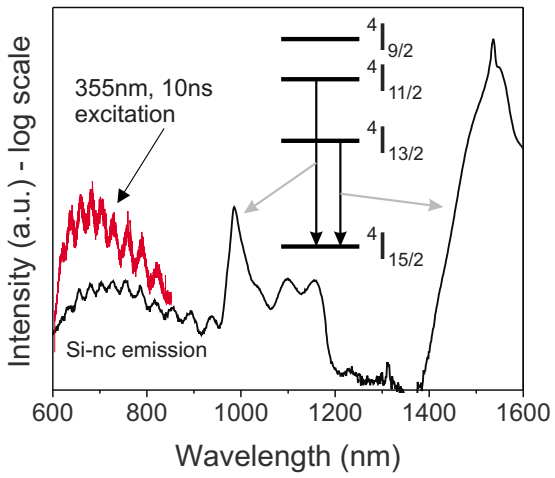

FIG. 1. (Color online) 4cw-PL spectrum of a typical SRO:Er sample under nondirect excitation (476 nm). The schematic structure of Er^{3+} electronic levels is reported. The red curve refers to the visible Si-np PL band obtained under 355 nm pulsed excitation (not in scale).

fluxes on the sample was about 1×10^{18} ph/(cm^2 s). The pulsed source was the third harmonic (355 nm) of a Nd:YAG laser with 10 ns pulse width, a repetition rate of 10 Hz and a photon flux of 1×10^{25} ph/(cm^2 s) during the pulse. For detection in the visible we have used a charge coupled device streak camera coupled to a spectrometer, with an overall time-resolution of the order of few picoseconds, and a monochromator coupled with a GaAs-photomultiplier (PMT), respectively, for time resolved (TR) and cw measurements. In the infrared, the signal was spectrally resolved with a monochromator and subsequently detected with a InGaAs IR-PMT. All measurements have been performed at room temperature.

A typical PL spectrum of our samples, measured with an excitation wavelength nonresonant with any Er^{3+} internal transition (476 nm), is shown in Fig. 1. It is possible to recognize several spectral features: around 980 and 1535 nm, the characteristic transitions of Er^{3+} in SiO_2 appear, related, respectively, to the first and second excited to the fundamental state optical transitions. The wide band centered at 700 nm is related to Si-np emission,[23] while the emission band at about 1100 nm is due to the Si substrate. When the sample is excited at 355 nm, the peak of Si-np PL band top is blue-shifted due to a different absorption cross section. This is reported as additional information in Fig. 1. However, the recombination dynamic is similar to the one investigated at 476 nm (more on this in Sec. III).

To get some insights about how the energy transfer is related to the nature of Si-np, whether they are amorphous[15] or crystalline, we have performed experiments in the IR range on reannealed samples A-re and B-re. It is worth to note that these measurements can be compared with literature reports where different time-scales for the transfer have been reported (fast—to the first excited state and slow—to higher Er^{3+} levels).[7,8]

Figure 2 summarizes the normalized TR-IR and cw-PL measurements for the samples A-re and B-re. The possibility of Er^{3+} clusterization during the annealed procedure has been discarded by analyzing the ions first excited state decay at

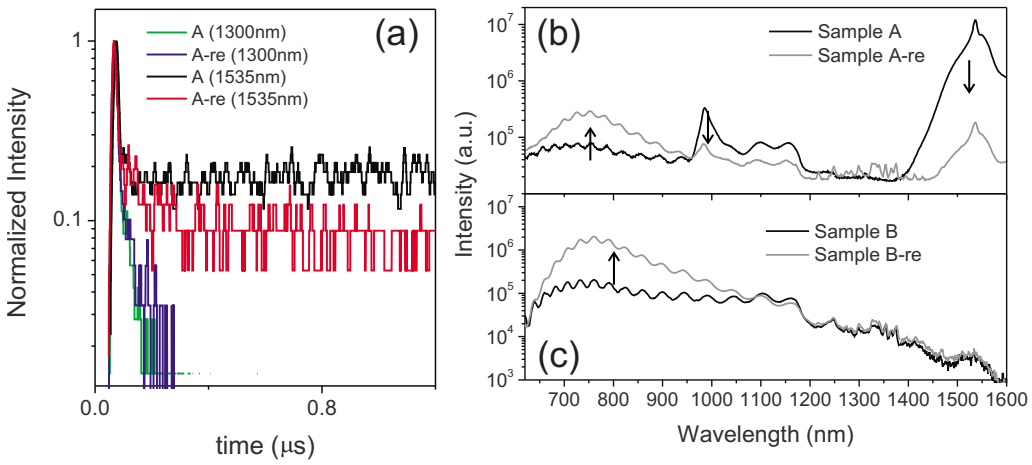

FIG. 2. (Color online) (a). TR-PL at different wavelengths for Sample A and B before and after the extra-annealing procedure. It is worth to note the presence of the same fast decay in the whole sample set. (b) Nonresonant cw broad-range PL spectra (λ_{exc}=476 nm) for the whole sample set. The extra-annealing induces an increase in the Si-np related emission together with a decrease in Er-related emission.

different pump fluxes, (as done in Ref. 24 for the preannealed samples). The results are very similar to those reported in Ref. 15, where samples A and B were investigated. In particular a fast decaying lineshape is observed in all the samples, with or without Er^{3+} and with or without the extra-annealing treatment. Inspecting the normalized decay kinetics [Fig. 2(a)], we observe a similar behavior for samples A and A-re. The fast emission looks independent from the Si-np nature (amorphous or crystalline). This suggests that this fast emission is due to matrix-related recombination centers, which are not affected by the reannealing process. This further confirms that this fast decay is not related to Auger back-transfer mechanism between excited Er^{3+} ions and Si-np. The transfer dynamics looks like it is not affected by the second annealing, since all the features presented in Ref. 15 are well reproduced even in the spectroscopic data obtained with these samples. From a more quantitative point-of-view, Figs. 2(b) and 2(c), reports a comparison between cw-PL of preannealed and reannealed samples. We can observe that an increase in the visible emission of Si-np and a decrease in the infrared emission of Er^{3+} are obtained by increasing the crystallinity degree of the samples. Particularly important is the more than one order of magnitude decrease in the Er^{3+} emission in sample A-re with respect to sample A: since this experiment has been performed with a cw excitation wavelength which is nonresonant with any Er internal transitions, we correlate this result with a less efficient energy transfer process in the reannealed sample. This will be confirmed in the model that will be detailed afterwards, where a faster transfer time for amorphous Si-np (~40 ns) has been found with respect to the reannealed samples (~120 ns).

III. VISIBLE PL SPECTROSCOPY

Samples A and B have been annealed for 1 h at 900 °C and likely contain amorphous nanoclusters with partial crystallization.[22] Nevertheless when excited with a cw laser, both emit a strong PL band centered at about 750 nm as shown, for example, in Fig. 1. On the other hand, once reannealed at 1100 °C, the phase separation between silicon and silicon oxide is improved and nanoparticles with high crystalline quality are formed. As suggested, for example by Fujii *et al.*,[25] the degree of sample crystallinity can be inspected analyzing the decays of the PL band in the visible. Figure 3 reports the VIS-TR-PL for different collection wavelengths for sample B before and after the extra-annealing process. The long decay curves in Fig. 3 are well fitted by a stretched exponential decay function, which takes into account distribution of lifetimes due to excitonic trans-

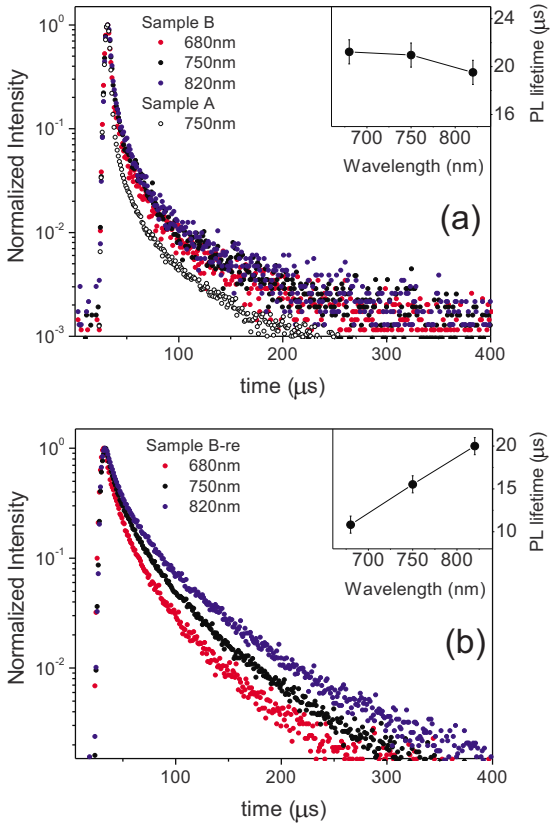

FIG. 3. (Color online) TR-PL decays for the sample without Er^{3+} [sample B (a) and B-re (b)] in logarithmic scale, in the 400 μs temporal window. The lifetimes obtained from the stretched exponential fits at various wavelengths are reported in the insets. When erbium is placed inside the sample, Si-np radiative recombination lifetime shortens significantly, as shown by comparing the decays at 750 nm for sample A [(a)—white circles] and B.

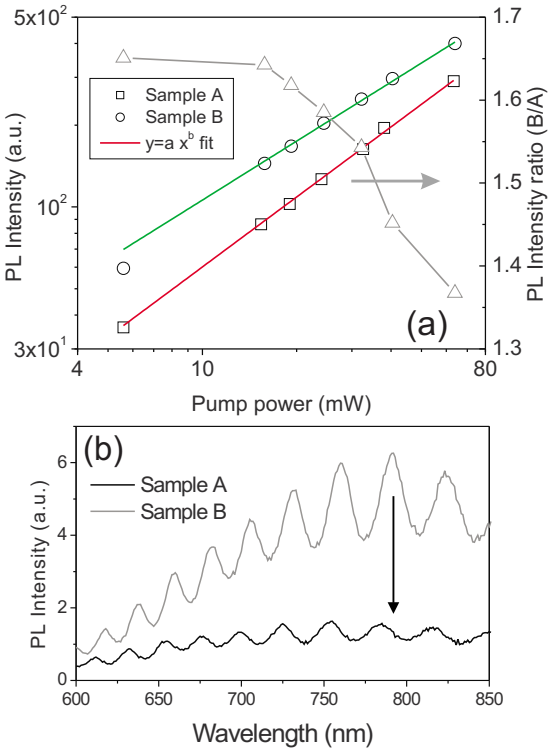

FIG. 4. (Color online) (a) Visible cw-PL intensity as a function of pumping power. The integrated intensity over the whole spectrum is fitted with a power-law $y=a\cdot x^b$ function, obtaining $b=0.83\pm0.05$ ($b=0.72\pm0.01$) for sample A (sample B). The intensity ratio of the two samples is added for clarity. (b) visible cw-PL spectra for sample A and B.

port phenomena, like interparticle hopping.[26,27] By fitting the data, the average PL lifetime τ_{PL} is extracted as the first-order moment of the stretched exponential distribution[28]

$$f(t)=e^{\{-((t-t_0/\tau))^{\beta}\}},\quad \tau_{PL}=\frac{\tau}{\beta}\Gamma\left[\frac{1}{\beta}\right], \tag{1}$$

where Γ is the Gamma-function. We clearly observe in the insets in Fig. 3 that while in sample B the lifetime is almost independent of the observation wavelength, in the extra-annealed sample B-re it shows a net trend, shortening at higher observation energies. The latter behavior is typical of exciton recombination in crystalline Si-np.[25,26] This is a confirmation of the different crystalline quality of the samples due to the different annealing temperatures.

Inspecting Fig. 3, a very fast decay (first few microseconds) is observed which is attributed to Auger recombination within the nanoparticle.[29] To check this hypothesis, we have measured the visible PL intensity of samples A and B as a function of excitation photon flux Φ. The results are reported in Fig. 4(a). The measurements have been fitted with a power-law function $I(\Phi)=a\cdot\Phi^b$. For sample B the power coefficient b is found to be very close to 2/3 ($b=0.72\pm0.01$), which is the signature of a three particle Auger recombination mechanism.[29] Although emission from sample B is more intense [triangle-dotted line in Fig. 4(a)], the power coefficient is higher for sample A ($b=0.83\pm0.05$). We explain these different exponents by the existence of a different mechanism in sample A that has reduced the population of the emitting level to values where Auger processes are weaker than in sample B and, thus, the exponent is closer to unity. The exciton population in sample A is lower than in sample B. We correlate this population depletion mechanism to the transfer process that competes with the intraband Auger recombination mechanism (more in Sec. IV).

Further proofs of energy transfer mechanism can be observed in the VIS-PL of Er^{3+} codoped samples.

- The whole luminescence band is quenched by a factor $\simeq$3.3 [900 °C annealed samples, Fig. 4(b)] and of a factor $\simeq$2.8 (extra-annealed samples, not shown);
- The PL lifetime shortens [shown, for sample A, as white circles in Fig. 3(a)]. This means that the transfer mechanism and radiative recombination are at least indirectly competitive processes, as will be carefully discussed in Sec. IV.

It is worth to note that in addition to the Si-np emission band in the visible, we have detected a broad weak emission that extends to the near IR, reaching almost 1600 nm, under cw excitation [see Fig. 2(b)]. Even if the origin of this emission is still unknown, we observe the following interesting aspects.

- This emission is quenched when Er^{3+} is inserted by about the same factor as the visible emission related to Si-np;
- the spectral lineshape of this band seems to be coincident with those of the fast decay reported in Ref. 15.

Based on these facts we hypothesize that the emission could be related to the presence of Si-np inside the matrix, even if the nanoparticles could be not directly responsible for the emission itself. Tentatively, it can be assigned to the centers reported in Ref. 30.

IV. RATE EQUATION SEMIEMPIRICAL MODELING

While the optical properties of Er ions in different matrices are well known, a careful study of the optical properties of Si-np can be performed only with extreme difficulty. The current fabrication processes do not allow a precise control of the particles geometry at the nanoscale, producing an ensemble of nanoparticles with different sizes and geometries. Moreover a long debate exists about the origin of the luminescence in Si-np: it can originate from intrinsic properties of the nanoparticles (quantum-confinement PL) or from localized recombination at the Si-np surface.[31] All these effects make the modeling of electronic and optical properties of Si-np a very difficult challenge, which can be successfully performed only for an ideal system. For this reason, we have chosen to follow a more empirical approach, in which the optical properties of the system are theoretically described by phenomenological rate equations. The kinetic of the populations is determined by a set of coupled rate equation which we have numerically solved to model the experimental data. Since the main recombination paths of Si-np are identified as Auger recombination within the nanoparticle and transfer to nearby Er ions, the fast dynamics of these two

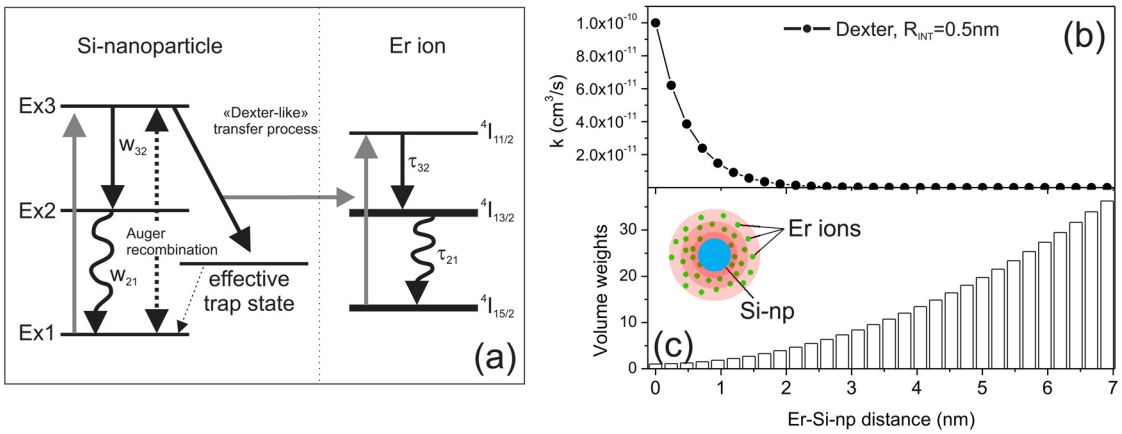

FIG. 5. (Color online) (a) Energy level scheme on which the rate equation system of Eq. (2) has been built. (b) Er–Si nanoparticle distance dependent coupling constants k_i which fits the experimental decay curve of sample A (Dexter-transfer). The parameter R_{int} has been taken from Refs. 12 and 43. (c) Weights in the average (4) which take into account the different Er ions number in different shell volumes.

processes make necessary a careful investigation of the experimental PL decay in the first few nanoseconds.

The following six-coupled equations system has been considered to model the Si-np/Er interaction[32]

$$\frac{d}{dt}N_{exc,1} = -\sigma_{\text{Si-np}}\Phi(t)N_{\text{Si-np}} + 0.5C_A(N_{exc,2})^3,$$

$$\frac{d}{dt}N_{exc,2} = w_{32}N_{exc,3} - C_A(N_{exc,2})^3,$$

$$\frac{d}{dt}N_{exc,3} = \sigma_{\text{Si-np}}\Phi(t)N_{\text{Si-np}} - w_{32}N_{exc,2} + 0.5C_A(N_{exc,2})^3 - kN_{exc,3}N_{\text{Er},1},$$

$$\frac{d}{dt}N_{\text{Er},1} = -kN_{exc,3}N_{\text{Er},1} + 1/\tau_{21}N_{\text{Er},2},$$

$$\frac{d}{dt}N_{\text{Er},2} = 1/\tau_{32}N_{\text{Er},3} - 1/\tau_{21}N_{\text{Er},2},$$

$$\frac{d}{dt}N_{\text{Er},3} = kN_{exc,1}N_{\text{Er},3} - 1/\tau_{32}N_{\text{Er},3}. \quad (2)$$

The Si-np excitonic levels are described by a three effective levels scheme (Ex1, Ex2, Ex3 of population $N_{exc,1}$, $N_{exc,2}$, $N_{exc,3}$, respectively), while for the Er ions we have considered the electronic population of level $^4I_{15/2}$ ($N_{\text{Er},1}$), $^4I_{13/2}$ ($N_{\text{Er},2}$), and $^4I_{11/2}$ ($N_{\text{Er},3}$). The corresponding energy level scheme is reported in Fig. 5(a). The other symbols in Eq. (2) have the following meaning.

- $\sigma_{\text{Si-np}}$, $\Phi(t)$, and C_A are, respectively, the Si-np absorption cross section ($\sim 1\times 10^{15}$ cm^2,[33]), the pump flux at excitation wavelength (355 nm) and the Auger coefficient. The pump flux temporal shape is a Gaussian function with full width half maximum estimated from the experimental data (10 ns).
- w_{ij} is the probability of the $i \rightarrow j$ transitions while τ_{ij} is the inverse of the transition probability.[34]
- k is the distant dependent coupling constant for the energy transfer process among Si-np and Er ions.

The *geminate* and *nongeminate* recombination terms ($\propto N_{exc,2}$ and $\propto N^2_{exc,2}$) have been neglected, since the Si-np excitonic levels population dynamic is dominated by Auger and energy transfer mechanisms in the first tens of nanoseconds after the excitation has been turned off.

Once an exciton has been formed in level Ex3 by absorbing the 355 nm photons, it can relax either to level Ex2 with a probability w_{32} or to an internal effective-trap-state by giving back the energy to an Er ion which gets excited. If relaxation to level Ex2 occurs, the carrier can be re-excited back to level Ex3 by an Auger process (which has been modeled with the terms $C_A(N_{exc,2})^3$) or alternatively can radiatively recombine to the level Ex1, emitting photons responsible for the Si-np emission band reported, for example, in Fig. 2.

The energy transfer process is accompanied by the promotion of one electron from the Er^{3+} fundamental state $^4I_{15/2}$ to the second excited state $^4I_{11/2}$ from which it can relax through Er^{3+} internal recombination channels with a time τ_{32}, as reported in Ref. 15.

It is worth to note the importance of Auger process in "recycling" the electrons to high lying Si-np levels, from which they can transfer their energy to nearby Er ions. In this scheme, radiative recombination of population $N_{exc,2}$ and energy transfer can be seen as indirectly competing mechanisms.

Excitons from the effective trap level cannot recombine radiatively so they are considered totally inactive in terms of VIS-PL emission [this has been indicated with a dashed arrow relaxation term in Fig. 5(a)]. The existence of a "traplike" state, through which Si-np sensitizes Er^{3+} ions, has been a recurring idea in several models of energy exchange mechanism.[35–39] Direct experimental evidences of their existence have been recently obtained for Er^{3+} doped bulk Si.[40] Actually, there is still some debate about the existence of the physical origin of this state in Er-doped SRSO material. In addition, some groups claim the existence of "traplike" states originating from defects in the SiO_2 matrix and not corre-

lated with Si-np.[41,42] Since it is out of the scope of this paper the investigation of the nature of this "trap-state," we limit ourselves to hypothize its existence. We model it as an effective level which is strongly correlated with the presence of Si-np. The effective trap level explains the decrease in the whole VIS-PL spectra when Er ions are added in the SRO matrix [see Fig. 4(b)]. In fact, a pure resonant transfer model would imply important differences in the spectral shape of visible emission comparing samples with and without Er^{3+}, since depletion of emission should occur at the energy of the resonant levels. The introduction of the effective trap level poses the transfer mechanism (resonant process) competing with the radiative recombination through Auger effects (nonresonant process), realizing a broad band quenching of the whole visible PL emission.

It is worth to note that some other works[41,42] support the existence of a different kind of traplike states ["luminescent centers" (LCs)] present in the SiO_2 matrix, which are related to the energy transfer mechanism among Si-np and Er ions. However, the LC derived transfer scheme is different from the excitonic related one which we propose in this manuscript. Indeed, our VIS-PL spectroscopic data strongly differ from the one attributed in literature to LCs. On one side, we did not measure any luminescent band centered at 550 nm, which could be attributed to LC mediated PL (Ref. 41) in our samples; on the other side we always detect long PL recombination lifetimes ($\sim$100 μs) at odds with the very fast one attributed to LC (tens of nanoseconds, as reported in Refs. 41 and 42). Moreover, both the PL lifetime shortening [Fig. 3(a)] and the reduction in Auger related power-law coefficient [Fig. 4(a)] when Er is inserted in the samples point toward a energy transfer process which has to compete, at least indirectly, with the Si-np excitonic radiative recombination. So, we attribute the main role of energy transfer to the Si-np, having no evidences of the presence of LC in our samples.

The probability that a transfer occurs is proportional to the coupling constant k, which itself is strongly dependent from the distance between Er ions and Si-np. As reported in different works,[11,12,18,43] the coupling constant scales with distance following an exponential decay law: this is a clear signature of an electronic exchange mechanism between donor and acceptor generating from wave function overlap (Dexter transfer).[16] The other possible transfer mechanisms, dipole-dipole interaction (Förster) and indirect radiative excitation do not likely occur in our system: the former being too slow with respect to the fast transfer time we measured (tens of nanoseconds), while the latter does not explain the enhancement of Er ions effective excitation cross section, being less efficient than direct excitation itself. Since Dexter mechanism is strongly dependent from interaction distance, we have considered a shell-model to reproduce the experimental data with numerical simulations. In this framework, we have worked under the assumptions of spherical nanoparticles surrounded by an homogeneous distribution of Er ions. For a fixed distance between the Si-np and Er^{3+}, r_i, we have defined an interaction shell, characterized by a coupling constant k_i, which depends on the distance according to

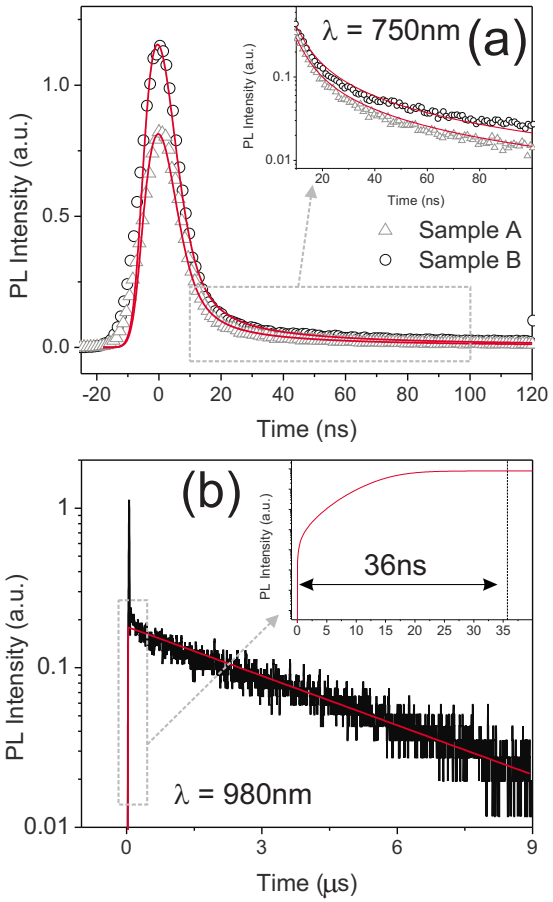

FIG. 6. (Color online) (a) Fit of experimental TR-PL data at 750 nm using the $N^{tot}_{exc,2}(t)$ population solution of system (2) in amorphous nanoclusters samples (A and B) in a 140 ns time window. The inset shows a zoom of the decay in logarithmic scale. (b) Fit of experimental TR-PL data at 980 nm of sample A using $N_{Er,3}(t)$ population solution of system (2). Inset: Si-np to Er^{3+} transfer time estimation.

$$k_i = k_0 e^{\{-(r_i - R_{\text{Si-np}})/R_{int}\}}, \tag{3}$$

where k_0 represents the maximum coupling constant value, when Er is placed exactly on the Si-np surface and $R_{\text{Si-np}}$ is the Si-np radius. The value of the constant R_{int} (characteristic interaction distance) has been taken from literature and it is equal to 0.5 nm (2.1 nm) for amorphous Si-nanoclusters[12,43] (Si-nanocrystals[17]). Clearly, this simple model can be applied reliably only for Er-Si-np distances smaller than some nanometers, where it is possible to consider interaction among only one *single* Si-np and many Er ions.

The high pumping fluxes used in the TR-PL experiments lead to a regime in which multiexcitons have been created inside the nanoparticles (this is confirmed by the power-law fits in Fig. 4). In fact, the maxima of the curves reported in Fig. 6(a) correspond to a local excitonic density of about $1-2\times10^{20}$ cm^{-3} ($\sim$4–5 excitons within the nanoparticle, where an average nanoparticle size of 4 nm diameter has been assumed). In this situation, which lasts for tens of nanoseconds before relaxing to single-exciton regime, we can correlate the PL intensity with the square of the Si-np electronic population which we get from numerical solutions of Eq. (2).[29]

The procedure we used for the fit is based on the as-

sumption that apart from the transfer, the recombination dynamics of Si-np is not affected by the presence of Er. Thus we initially fitted the luminescence decay for the sample without Er (sample B) with the constraint $k=0$. In this way we determined the parameters w_{ij} and C_A. Then, the transfer process is considered by using these values as starting guesses for the Si-np recombination dynamics, while we fitted the sample A decay curve to determine the transfer properties. Er recombination parameters (τ_{32} and τ_{21}) and Si-np PL lifetime (w_{21}^{-1}) have been taking from experimental data and are equal, respectively, to 4.2 μs, 5.5 ms, and 21 μs, as reported in Ref. 15 and Sec. III. To take into account the distance dependent coupling constant, we sum-up a weighted average of the solutions at each interaction distance. To this end, we considered the ith-shell which is distant r_i from the Si-np, and thus characterized by a coupling constant k_i. To take into account the different number of Er ions in shells of different volume, the solutions $N_{exc,2}^{i}(t)$ for each shell i have been weighted

$$N_{exc,2}^{\mathrm{tot}}(t) = \frac{\sum_{i=1} N_i \cdot V_i}{\sum V_i}, \tag{4}$$

to yield the value $N_{exc,2}^{\mathrm{tot}}(t)$. The weight V_i represents the different number of Er ions accessible for different Er-Si-np distances (different shell volumes, proportional to $r_{i+1}^3 - r_i^3$).

The values of coupling constants k_i which fit the experimental decay curve of sample A in a 140 ns time window are reported in Fig. 5(b) (black circles), as a function of Er-Si-np distances r_i ($k_i=[0.1\times10^{-16}-0.8\times10^{-10}]$ cm^3/s). The interaction distance corresponding to the lowest k_i is equal to about 7 nm. It is very important to point out that this value is the distance needed to reproduce the experimental data: indeed, the Dexter transfer abruptly decreases with distance and only the Er^{3+} ions placed at a distance smaller than 2–3 nm greatly contribute to modify the Si-np recombination dynamic. Clearly, the other distant ions have a small or negligible coupling with the Si-np, yet they have to be included to reproduce the observed decays. Finally, Fig. 5(c) reports the V_i values estimated for this specific case.

Figure 6 reports the final results of the fits. The intraband recombination probabilities have been found to be $w_{32}=1\pm2\times10^{10}$ and $1\pm3\times11^{10}$ s^{-1}, while the Auger coefficients $C_A=2\pm3\times10^{-32}$ and $C_A=1\pm2\times10^{-33}$ cm^6/s, for amorphous nanocluster and nanocrystalline samples, respectively. Even with this simple model, the numerical results reproduce qualitatively the experimental data, being the correlation coefficient of the fitting, R^2, of 0.99 for both amorphous nanoclusters samples.

This model allows to explain most of the experimental data such as the reduction in the whole Si-np emission band or the lifetime shortening of the PL visible emission, when Er^{3+} is inserted in the samples. This last phenomenon can be understood by the role of Auger processes. The energy transfer becomes an indirect competing mechanism with the radiative recombination of the level Ex2, due to Auger carrier "recycling" from level Ex2 to level Ex3. Excitons in this last level can eventually relax very fast in the effective trap level, exciting an Er ion without relaxing again to the level Ex2, contributing to a fast level depletion mechanism.

Similar results have been obtained for re-annealed samples, with a R^2 of 0.96 and 0.88 for sample A-re and B-re, respectively. In this case, the longer interaction distance (2.1 nm) for Si-nanocrystals than for Si-nanoclusters makes the model less reliable, since it is necessary to introduce large Er-Si-np distances ($\sim$15–20 nm, in comparison with 6–7 nm for nanoclusters) to reproduce the experimental data. For these distances the hypothesis of a single nanoparticle interacting with many Er ions cannot be strictly verified. The range of coupling constant obtained, $k_i=[5\times10^{-10}-1\times10^{-9}]$ cm^3/s, has to be intended as a guess of the actual values. Nevertheless, good fit of the decay lineshapes for all the samples employing the same rate equations validate the hypothesis of the existence of a single kind of energy transfer mechanism.

The larger transfer efficiency of nanoclusters with respect to nanocrystals is interpreted considering the different characteristic interaction distances (R_{int}), which translates, for large shells, in a low transfer probability which can be eventually overcome by Auger mechanisms. It is also possible that the annealing process have influenced the spatial distribution of Si-np inside the matrix, changing the number of Er ions close to the nanoparticle surface.

Once all the parameters in Eq. (2) have been evaluated, it is possible to estimate the average transfer time between Si-np and Er ions inspecting the rise of the population $N_{\mathrm{Er},3}$. Figure 6(b), reports the experimental data for sample B at 980 nm (level $^4I_{11/2}$), which is reproduced by correlating the PL signal with the $N_{\mathrm{Er},3}(t)$ population. The "slow" decay due to Er^{3+} internal relaxation is well reproduced, while the rise, even if experimentally hidden by the fast-decaying peak discussed in Ref. 15, shows a good compatibility between numerical and experimental results. This means that the characteristic rise time is shorter than 100 ns. The inset of Fig. 6(b), shows a zoom of the first nanoseconds of the curve, from which a transfer time of 36 ± 10 ns can be extracted. This value is characteristic of amorphous clusters. For nanocrystalline samples, we extracted an average transfer time of 117 ± 30 ns. It was found also that, while the fit parameters C_A and k are strongly dependent from the number of excitons within the nanocrystal after the laser excitation, the transfer time itself has revealed to be quite robust with respect to different initial conditions, such as different Si-np diameters or average concentrations.

V. CONCLUSIONS

In conclusion, we have presented spectroscopic experimental results on a set of Er-doped silicon-rich-silicon-oxide samples, with amorphous or crystalline Si-np. These samples are particularly interesting since they show the highest to date fraction of Er ions coupled to Si-np ($\sim$52%),[13] which produces an internal gain in waveguide samples of about 1 dB/cm.[14] In this study, we have demonstrated that the physics behind the transfer mechanism does not depend on the Si-np nature; in particular, we have verified that Auger back transfer processes are negligible in crystalline Si-nc samples,

confirming the previous results obtained in amorphous Si-np.[15] The study of the emission from the Si-np has allowed us to suggest a physical model for the energy transfer mechanism. In this scheme, the main issue to be addressed in achieving an efficient Si-np—Er^{3+} coupling is the distance-dependent transfer. Even if the same model apply to different Si-np phases (amorphous or crystalline), the transfer efficiency appears to be larger for amorphous Si-nanoclusters than for nanocrystals, showing a more than one order of magnitude increase in the Er^{3+} emitted PL intensity when pumped non-resonantly at the same photon flux. This is explained by a faster transfer rate from amorphous than from crystalline nanoparticles. The very fast transfer was modeled with a process which is competitive with the overall recombination dynamics of the Si-np. The model predicts the presence of an intermediate energy level which we labeled effective trap and whose origin is still under debate. This level allows the separation of the internal Si-np dynamics from the transfer and allows explaining most of our experimental results. An important finding of this work is the role played by Auger recombination in the Si-np which allows to recycle a fraction of the excitons in Si-np to contribute to the energy transfer.

We believe that our findings allow reconsidering the whole Er-Si-np system and give a direction for further improving this material system to reach the conditions for complete inversion and thus to realize amplifiers or lasers.

ACKNOWLEDGMENTS

The authors acknowledge EU commission funding through project Lancer (Grant No. FP6—033574 and Helios (Grant No. FP7-224312).

[1]P. C. Becker, N. A. Olsson, and J. R. Simpson, *Erbium-Doped Fiber Amplifiers: Fundamental and Technology* (Academic, New York, 1999).
[2]A. Polman and F. C. J. M. van Veggel, J. Opt. Soc. Am. B **21**, 871 (2004).
[3]A. J. Kenyon, P. F. Trwoga, M. Federighi, and C. W. Pitt, J. Phys. Condens. Matter **6**, L319 (1994).
[4]F. Priolo, G. Franzò, D. Pacifici, V. Vinciguerra, F. Iacon, and A. Irrera, J. Appl. Phys. **89**, 264 (2001).
[5]F. Iacona, D. Pacifici, A. Irrera, M. Miritello, G. Franzò, and F. Priolo, Appl. Phys. Lett. **81**, 3242 (2002).
[6]H. Han, S. Seo, and J. Shin, Appl. Phys. Lett. **79**, 4568 (2001).
[7]I. Izeddin, A. S. Moskalenko, I. N. Yassievich, M. Fujii, and T. Gregorkiewicz, Phys. Rev. Lett. **97**, 207401 (2006).
[8]I. Izeddin, D. Timmerman, T. Gregorkiewicz, A. S. Moskalenko, A. A. Prokofiev, I. N. Yassievich, and M. Fujii, Phys. Rev. B **78**, 035327 (2008).
[9]M. Wojdak, M. Klik, M. Forcales, O. B. Gusev, T. Gregorkiewicz, D. Pacifici, G. Franzò, F. Priolo, and F. Iacona, Phys. Rev. B **69**, 233315 (2004).
[10]P. G. Kik and A. Polman, J. Appl. Phys. **88**, 1992 (2000).
[11]B. Garrido, C. García, S.-Y. Seo, P. Pellegrino, D. Navarro-Urrios, N. Daldosso, L. Pavesi, F. Gourbilleau, and R. Rizk, Phys. Rev. B **76**, 245308 (2007).
[12]D. Navarro-Urrios, N. Daldosso, C. García, P. Pellegrino, B. Garrido, F. Gourbilleau, R. Rizk, and L. Pavesi, Jpn. J. Appl. Phys., Part 1 **46**, 6626 (2007).
[13]D. Navarro-Urrios, Y. Lebour, O. Jambois, B. Garrido, A. Pitanti, N. Daldosso, L. Pavesi, J. Cardin, K. Hijazi, L. Khomenkova, F. Gourbilleau, and R. Rizk, J. Appl. Phys. **106**, 093107 (2009).
[14]A. Pitanti, D. Navarro-Urrios, R. Guider, N. Daldosso, F. Gourbilleau, L. Khomenkova, R. Rizk, and L. Pavesi, Proc. SPIE **6996**, 699619 (2008).
[15]D. Navarro-Urrios, A. Pitanti, N. Daldosso, F. Gourbilleau, R. Rizk, and L. Pavesi, Phys. Rev. B **79**, 193312 (2009).
[16]D. L. Dexter, J. Chem. Phys. **21**, 836 (1953).
[17]K. Choy, F. Lenz, X. X. Liang, F. Marsiglio, and A. Meldrum, Appl. Phys. Lett. **93**, 261109 (2008).
[18]B. Garrido, C. García, P. Pellegrino, D. Navarro-Urrios, N. Daldosso, L. Pavesi, F. Gourbilleau, and R. Rizk, Appl. Phys. Lett. **89**, 163103 (2006).
[19]L. Khomenkova, F. Gourbilleau, J. Cardin, and R. Rizk, Physica E (Amsterdam) **41**, 1048 (2009).
[20]For deposition parameters is intended: the substrate temperature, the rf power on targets and the hydrogen rate in the hydrogen–argon mixture.
[21]N. Daldosso, M. Luppi, G. Dalba, L. Pavesi, F. Rocca, F. Priolo, G. Franzò, F. Iacona, E. Degoli, R. Magri, and S. Ossicini, Mater. Res. Soc. Symp. Proc. **770**, I1.3.1 (2003).
[22]M. Zacharias, J. Heilmann, R. Scholz, and U. Kahler, Appl. Phys. Lett. **80**, 661 (2002).
[23]The oscillations reported in the PL spectrum are interference fringes due reflection from the Si substrate.
[24]D. Navarro-Urrios, A. Pitanti, N. Daldosso, F. Gourbilleau, L. Khomenkova, R. Rizk, and L. Pavesi, Physica E (Amsterdam) **41**, 1029 (2009).
[25]M. Fujii, K. Imakita, K. Watanabe, and S. Hayashi, J. Appl. Phys. **95**, 272 (2004).
[26]L. Pavesi and M. Ceschini, Phys. Rev. B **48**, 17625 (1993).
[27]J. Linnros, N. Lalic, A. Galeckas, and V. Grivickasb, J. Appl. Phys. **86**, 6128 (1999).
[28]M. N. Berberan-Santos, E. N. Bodunov, and B. Valeur, Chem. Phys. **315**, 171 (2005).
[29]R. M'ghaieth, H. Maaref, I. Mihalcescu, and J. C. Vial, Phys. Rev. B **60**, 4450 (1999).
[30]L. Khriachtchev, M. Räsänen, S. Novikov, and L. Pavesi, Appl. Phys. Lett. **85**, 1511 (2004).
[31]S. Godefroo, M. Hayne1, M. Jivanescu, A. Stesmans, M. Zacharias, O. I. Lebedev, G. Van Tendeloo, and V. V. Moshchalkov, Nat. Nanotechnol. **3**, 174 (2008).
[32]D. Pacifici, G. Franzò, F. Priolo, F. Iacona, and L. Dal Negro, Phys. Rev. B **67**, 245301 (2003).
[33]D. Kovalev, J. Diener, H. Heckler, G. Polisski, N. Künzner, and F. Koch, Phys. Rev. B **61**, 4485 (2000).
[34]To have a clearer notation, we have indicated the relaxation terms employing the decay probability (w_{ij}) for the Si-np and the lifetimes ($\tau_{ij}=w_{ij}^{-1}$) for the Er ions.
[35]R. Hull, *Properties of Crystalline Silicon* (Academic, New York, 1999).
[36]F. Priolo, G. Franzò, S. Coffa, A. Polman, S. Libertino, R. Barklie, and D. Carey, J. Appl. Phys. **78**, 3874 (1995).
[37]S. Y. Seo and J. H. Shin, Appl. Phys. Lett. **78**, 2709 (2001).
[38]A. J. Kenyon, M. Wojdak, I. Ahmad, W. H. Loh, and C. J. Oton, Phys. Rev. B **77**, 035318 (2008).
[39]J. Warga, R. Li, S. N. Basu, and L. DalNegro, Physica E (Amsterdam) **41**, 1040 (2009).
[40]I. Izeddin, M. A. J. Klik, N. Q. Vinh, M. S. Bresler, and T. Gregorkiewicz, Phys. Rev. Lett. **99**, 077401 (2007).
[41]O. Savchyn, F. R. Ruhge, P. G. Kik, R. M. Todi, K. R. Coffey, H. Nukala, and H. Heinrich, Phys. Rev. B **76**, 195419 (2007).
[42]O. Savchyn, R. M. Todi, K. R. Coffey, and P. G. Kik, Appl. Phys. Lett. **93**, 233120 (2008).
[43]F. Gourbilleau, R. Madelon, C. Dufour, and R. Rizk, Opt. Mater. **27**, 868 (2005).